The influence of turbid medium properties on object visibility in optical Kerr gated imaging

2014 Laser Phys. 24 015401

(http://iopscience.iop.org/1555-6611/24/1/015401)

IOP Publishing | Astro Ltd Laser Physics
Laser Phys. **24** (2014) 015401 (7pp) doi:10.1088/1054-660X/24/1/015401

The influence of turbid medium properties on object visibility in optical Kerr gated imaging

Pingping Zhan[1], Jinhai Si[1], Wenjiang Tan[1], Xin Liu[2], Bin Wu[1], Shichao Xu[1], Feng Chen[1] and Xun Hou[1]

[1] Key Laboratory for Physical Electronics and Devices of the Ministry of Education and Shaanxi Key Lab of Information Photonic Technique, School of Electronic and Information Engineering, Xi'an Jiaotong University, Xianning-xilu 28, Xi'an 710049, People's Republic of China
[2] Science and Technology on Electro-Optical Information Security Control Laboratory, Sanhe 065201, People's Republic of China

E-mail: tanwenjiang@mail.xjtu.edu.cn

Received 6 September 2013, revised 31 October 2013
Accepted for publication 1 November 2013
Published 10 December 2013

Abstract
In this paper, we demonstrate femtosecond optical Kerr gated imaging of an object hidden behind a highly turbid medium. The influence of turbid medium properties on image contrast has been investigated. Experimental and Monte Carlo simulation results show that for a given optical density, the image contrast of direct imaging without an optical Kerr gate decreases with the increase of the scattering particle size or the decrease of the thickness of the turbid medium. Compared with direct imaging, optical Kerr gated imaging has a better image contrast as it eliminates more scattered photons effectively. Qualitative comparisons between experiments and simulations show good agreement.

Keywords: Femtosecond laser, optical Kerr effect, turbid media

(Some figures may appear in colour only in the online journal)

1. Introduction

There exist multiple scattering interactions when light transits through a highly scattering turbid medium. The multiple scattering that most of the photons participate in will disturb the fidelity of the optical information that is carried by the imaging photons. This situation can occur in many cases, for example, inferior visibility through fog, imaging of embedded objects in turbid media, and so on. It is important to pick up the useful imaging information for objects hidden in a turbid medium. Generally, light propagating in a turbid medium can be divided into three parts: the ballistic photons, the quasi-ballistic photons and the scattered photons [1]. The ballistic photons travel in a straight line and carry the information on objects behind or inside the turbid medium. The quasi-ballistic photons are also called snake photons; they travel remaining close to their initial trajectory and also carry useful information about internal objects along their propagation [2, 3]. The scattered photons are those which undergo multiple scattering and provide no useful information. A small number of undisturbed 'ballistic' photons penetrate the turbid medium even in extreme scattering conditions. The essence of imaging through turbid media is to extract the information carried by the ballistic and quasi-ballistic photons.

The imaging quality of an object in a turbid medium can be improved by limiting the collection of the scattered photons. The general technique is known as 'time gated imaging' [4, 5], and makes use of a very fast shutter to select the ballistic and quasi-ballistic photons from the transmitted imaging photons. Most time gated imaging systems depend on the optical Kerr gate (OKG) technique [6–11]. The OKG is based on the optical Kerr effect, and its shutter time can be up to tens of femtoseconds. In recent decades, the time gated imaging technique based on the OKG has been used in biomedical research [12–14]. Recently, the time gated imaging technique has also been applied in investigating the dynamics of spray breakup and vaporization to overcome the strong scattering in the near field of the atomizing spray [15–20]. However, object visibility in time gated imaging is dependent on the optical properties of the spray, such as the diameter of the spray, the size of the scattering particles and the optical density. At different distances from the nozzle of the injector, the optical properties of the spray are different. Therefore, study of the influence of the optical properties of a spray on object visibility is significant.

In this paper, we demonstrate femtosecond optical Kerr gated imaging of an object hidden behind a highly turbid medium. The influence of turbid medium properties on image contrast has been investigated. The experimental results show that for a given optical density (OD), the image contrast of direct imaging decreases with increase of the scattering particle size or decrease of the thickness of the turbid medium. Compared with direct imaging, a better image contrast can be obtained by using optical Kerr gated imaging. Furthermore, we investigate the temporal and spatial evolution of the femtosecond pulse transmitted through the turbid medium by Monte Carlo (MC) simulations. The simulations show that a femtosecond pulse is spatially and temporally diffused more seriously when it is transmitted through a turbid medium with smaller scattering particles or larger thickness at the same OD. The simulations indicate that for a given OD, the image contrast of direct imaging without the use of an optical Kerr gate decreases with increase of the scattering particle size or decrease of the thickness of the turbid media. Moreover, a better image contrast can be obtained by using optical Kerr gated imaging as it eliminates more scattered photons effectively.

2. Experiments

A schematic of the ballistic imaging system in our experiments is shown in figure 1. A Ti:sapphire laser system (Coherent Inc., Libra-USP-HE) with a repetition rate of 1 kHz and a pulse duration of 50 fs at 800 nm was used in our experiments. The output beam was split into two beams by a short pass filter (SPF: Newport Inc., 10SWF-800-B). The transmitted short-wavelength part centered at about 780 nm was used as the gating beam and the reflective long-wavelength part centered at about 800 nm was used as the imaging beam. The imaging beam was modulated by a 1.41 1ine pair mm^{-1} section of the resolution test pattern (a United States Air Force contrast target) and then introduced into the turbid medium. The imaging beam transmitted from the turbid medium was collected by a lens (L2), and then passed through an ultrafast OKG. The OKG consisted of a pair of calcite-crossed polarizers with a Kerr medium between them. The Kerr medium was a CS_2 solution filled in a 1 mm glass cuvette. The gating beam passed through the optical delay line and was focused into the Kerr medium by the lens L1. The polarization direction of the gating beam was rotated by 45° by a half-wave plate for maximum gate efficiency. When the OKG was opened by the gating pulse, part of the imaging beam could pass through the analyzer. By adjusting

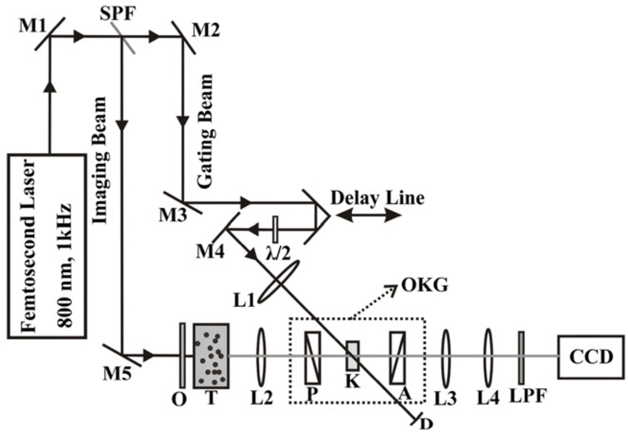

Figure 1. Schematic of the ballistic imaging system in our experiment. SPF, short pass filter; λ/2, half-wave plate; O, object; T, turbid medium; P, polarizer; K, optical Kerr material; A, analyzer; OKG, optical Kerr gate; D, dump; LPF, long pass filter; M1, M2, M3, M4 and M5, mirrors; L1, L2, L3 and L4, lenses.

the time delay between the gating pulse and the imaging pulse, the ballistic component of the imaging beam could be temporally picked out by the OKG. The optical Kerr gated imaging beam was subsequently collected by two lenses (L3, L4) and imaged onto a CCD camera (Nikon DXM 1200F). A long pass filter (LPF: Newport Inc., 10LWF-800-B) was placed between L4 and the camera in order to decrease the intensity of the noise generated by the pump pulse scattering in the optical Kerr medium.

In our experiments, we used three kinds of polystyrene microsphere suspensions as the turbid medium; the diameters of polystyrene microspheres were 0.4, 0.7 and 1.4 μm, respectively. The polystyrene microspheres (Sphere Scientific Co., Ltd) were stored as aqueous dispersions, the concentration of which was approximately 5% (w/v). The turbid media were prepared by diluting the aqueous dispersions of polystyrene microspheres with de-ionized water, and then sonicating at room temperature for 1 min. The ODs of the turbid media were adjusted by altering the concentrations of the aqueous dispersions of polystyrene microspheres, and measured by the collimated transmittance approach [9].

3. Results and discussion

An essential aspect of an optical system is its ability to transmit spatial information. The relevant parameter to evaluate performance is the visibility, or image contrast. Figure 2 shows images with and without the OKG and the corresponding intensity distributions for the suspensions of 0.4, 0.7 and 1.4 μm polystyrene microspheres, in which 1 cm-thick polystyrene microsphere suspensions at the same OD = 11 were used. From figure 2(a), we can see that the visibilities of the images without the OKG (here we call this direct imaging) decrease with increase of the size of the polystyrene microspheres. In direct imaging, the number of scattered photons is imaged as the noise, so the visibilities of the images are determined not only by the OD of the turbid medium, but also by various scattering properties. For

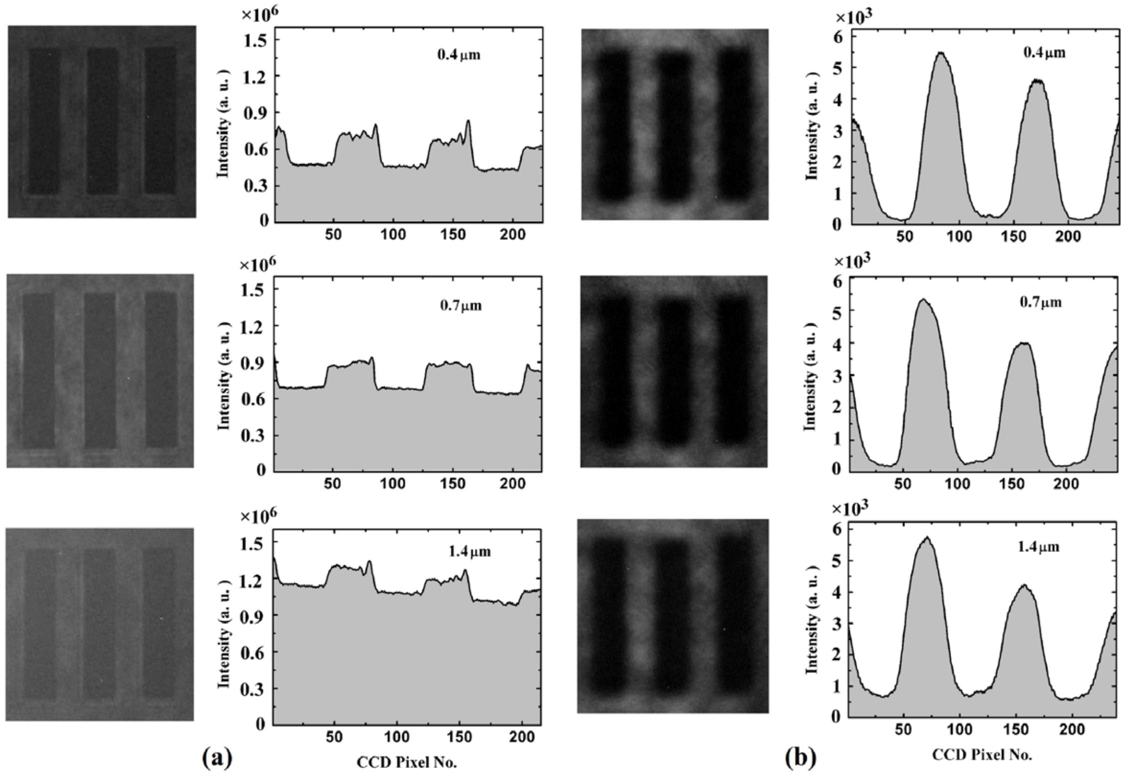

Figure 2. Images and corresponding plots of 1D (summed) intensity distributions obtained for the suspensions of 0.4, 0.7 and 1.4 μm polystyrene microspheres at the same OD = 11. (a) Direct imaging. (b) Optical Kerr gated imaging.

example, more scattered photons were imaged as noise for the suspension of 1.4 μm polystyrene microspheres, as shown in figure 2(a). In contrast, the visibilities and intensities of the images with the OKG (here we call this optical Kerr gated imaging) were nearly the same, as shown in figure 2(b), due to its excellent temporal filtering of the scattered photons.

Furthermore, to quantitatively investigate the influence of various scattering properties on the image contrast, we calculated the image contrast, which is defined as

$$\text{Contrast} = \frac{I_{\max} - I_{\min}}{I_{\max} + I_{\min}} \quad (1)$$

where $I_{\min}$ is the average light intensity corresponding to the shaded region and $I_{\max}$ is the average light intensity corresponding to the unshaded region of the imaged resolution test chart.

3.1. The influence of the particle size of the turbid medium on the image contrast

From figure 3(a), we can see that the image contrast of direct imaging decreases with increase of the scattering particle size at the same OD. In addition, the image contrast also decreases with increase of the OD of the turbid medium and approximately equals zero due to the increased scattered photons. Compared with direct imaging, optical Kerr gated imaging has a much better image contrast, as shown in figure 3(b). The reason is that more forward scattered photons through the turbid medium with larger scattering particles were collected at the same collecting angle when direct imaging was used. It also should be noted that CS_2 was used here as the optical Kerr medium. CS_2 has a slow response time of about 1.6 ps, which is larger than the time duration of the imaging pulse. Although the OKG could eliminate most of the scattered photons of the imaging beam, some residual forward scattered photons could also be imaged in our experiment. Therefore, the image contrast of optical Kerr gated imaging also decreases slightly with increase of the OD of the turbid medium, as shown in figure 3(b).

In addition, the corresponding image intensities for figure 3 were also measured as shown in figure 4. From figure 4(a), we can see that the image intensities for direct imaging of the turbid medium with larger scattering particles are larger than those for the turbid medium with smaller scattering particles at the same OD. However, the image intensities for optical Kerr gated imaging of the turbid media with different scattering particles are nearly the same and lower than those for direct imaging at the same OD, as shown in figure 4(b). The image intensities for optical Kerr gated imaging were well fitted by an exponential function. This exponential relationship conformed well to Beer's law and indicated that the scattered photons were isolated efficiently from the ballistic photons by the OKG. The results showed that a better image contrast could be acquired with optical Kerr gated imaging compared with direct imaging, which was consistent with the results for the image contrast shown in figure 3.

3.2. The influence of the thickness of the turbid medium on the image contrast

We also investigated the influence of the thickness of the turbid medium on the image contrast at different ODs.

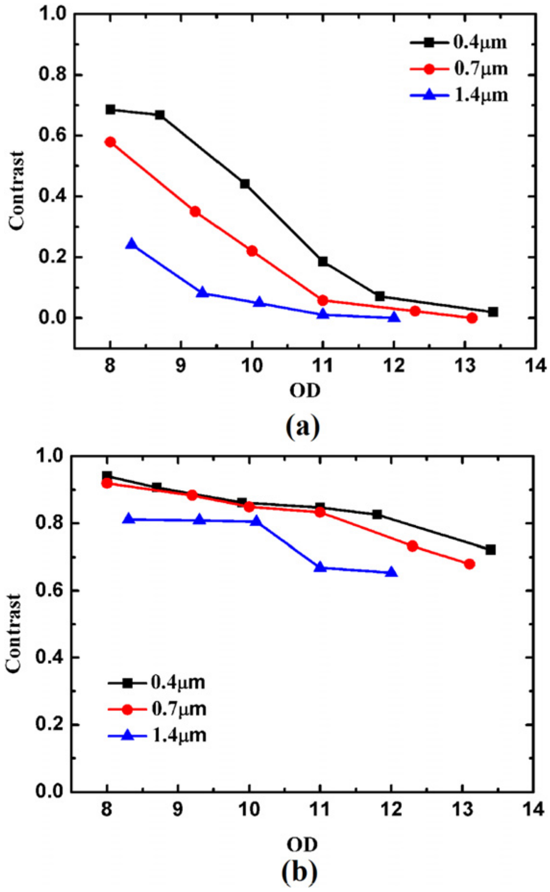

Figure 3. Image contrasts for the suspensions of 0.4, 0.7 and 1.4 μm polystyrene microspheres at different ODs. (a) Direct imaging. (b) Optical Kerr gated imaging.

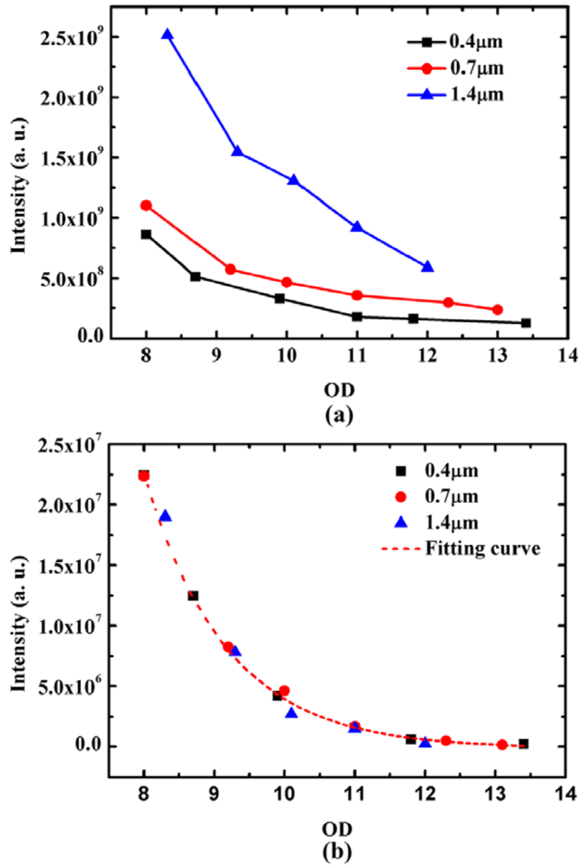

Figure 4. Image intensities for the suspensions of 0.4, 0.7 and 1.4 μm polystyrene microspheres at different ODs. (a) Direct imaging. (b) Optical Kerr gated imaging.

The turbid media were suspensions of 0.7 μm polystyrene microspheres, the thicknesses of which were 1 and 5 cm. As shown in figure 5(a), the image contrast of direct imaging for the thick turbid medium is better than for the thin turbid medium at the same OD. We also inferred that the number of forward scattered photons through a thinner turbid medium was more than that through a thicker turbid medium at the same OD. Compared with direct imaging, a better image contrast can be acquired with the OKG at the same OD, as shown in figure 5(b). As mentioned above, some residual forward scattered photons can be imaged by using the optical Kerr gate of CS_2 in our experiment. Therefore, it also can be seen from figure 5(b) that the image contrast of optical Kerr gated imaging for the thicker turbid medium was better than that for the thinner turbid medium.

Furthermore, we also measured the corresponding image intensities for figure 5. As shown in figure 6(a), the image intensities for direct imaging of the 1 cm-thick turbid medium were larger than those for the 5 cm-thick turbid medium at the same OD. Similarly to the results in figure 4(b), the image intensities for optical Kerr gated imaging of the turbid media of different thicknesses at the same OD were also nearly the same and well fitted by an exponential function. The results also confirmed that the image contrast of optical Kerr imaging can be better than the image contrast of direct imaging, as shown in figure 5.

3.3. Monte Carlo simulation

To further reveal the influence of the scattering particle size and the thickness of the turbid medium on the image contrast, we have also investigated the temporal and spatial evolution of a femtosecond pulse transmitted through a turbid medium by Monte Carlo simulations. The detailed description of the MC simulation technique for light propagating through a turbid medium can be found in [21, 22]. The optical parameters of the polystyrene microsphere suspensions given above were used in the simulation. Because the absorption of 800 nm light within the polystyrene microspheres was negligible, in our simulation, the refractive indices of the scattering particles (polystyrene microspheres) and the surrounding medium (distilled water) were set to 1.58 and 1.33, respectively. Moreover, the extinction coefficient μ_e equaled the scattering coefficient μ_s in our simulations. Also, the OD equaled the scattering coefficient μ_s times the thickness of the turbid medium l. The pulse duration and spatial width of the incident pulse were set to 50 fs and 0.58 cm, respectively. One billion photons were launched for the MC simulations.

Firstly, we simulated the temporal and spatial evolution of a femtosecond pulse transmitted through three kinds

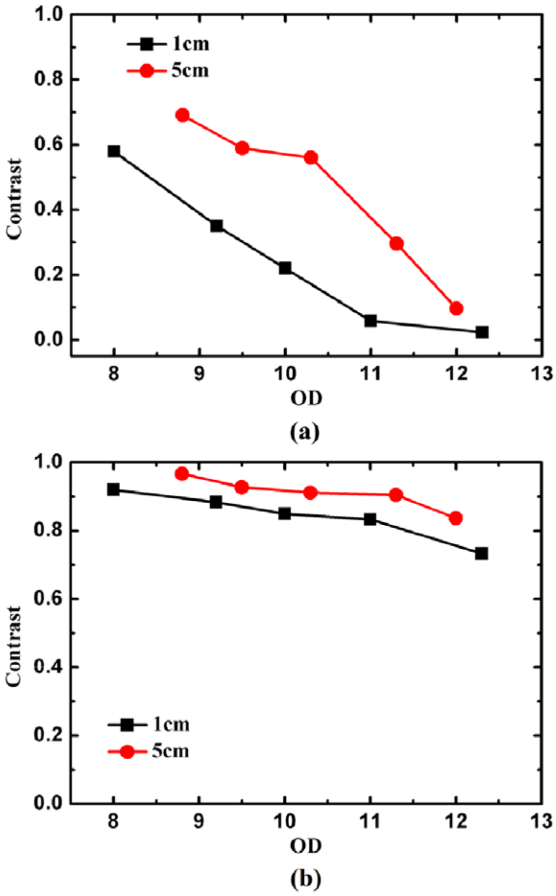

Figure 5. Image contrasts for the 1 and 5 cm-thick suspensions of 0.7 μm polystyrene microspheres at different ODs. (a) Direct imaging. (b) Optical Kerr gated imaging.

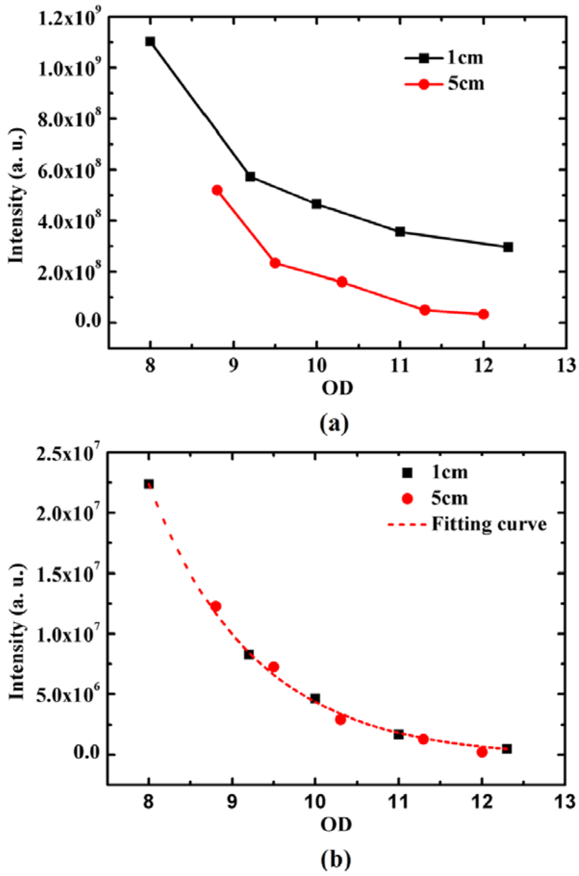

Figure 6. Image intensities for the 1 and 5 cm-thick suspensions of 0.7 μm polystyrene microspheres at different ODs. (a) Direct imaging. (b) Optical Kerr gated imaging.

of turbid media. The scattering particle sizes were set to 0.4, 0.7 and 1.4 μm. According to Mie theory [23], the anisotropy parameters of the three scattering particles were calculated to be 0.684, 0.845 and 0.927, respectively. The scattering coefficient μ_s and the thickness of the turbid medium l were set to be 10 cm^{-1} and 1 cm, respectively. Figure 7(a) shows the intensity distribution of the incident pulse and figures 7(b)–(d) show the intensity distributions of the transmitted pulse on the front faces of the turbid media. The FWHMs (full widths at half maximum) of the intensity distributions in figures 7(b)–(d) are estimated to be 1.3, 1 and 0.8 cm, for the turbid media of 0.4, 0.7 and 1.4 μm polystyrene microspheres, respectively. In addition, the number of transmitted photons collected on the front face increases with increase of the scattering particle size as shown in figures 7(b)–(d). As a result, when the size of the scattering particles is increased to 1.4 μm from 0.4 μm, the image contrast of direct imaging becomes low because the number of ballistic photons remains unchanged for the same OD.

Figure 7(e) shows the normalized temporal intensity profiles of the transmitted femtosecond pulse as shown in figures 7(b)–(d). From figure 7(e), we can see that the transmitted femtosecond pulse was broadened more by decreasing the scattering particle size. In our simulation, the temporal intensity profiles of the multiply scattered photons were spread over twenty picoseconds. Therefore, these multiply scattered photons could be eliminated temporally by the OKG, and the image contrast of optical Kerr gated imaging is better than the image contrast of direct imaging under the same conditions. However, if the gating time of the OKG was slightly longer than the temporal duration of the ballistic photons, more residual forward scattered photons could also be gated for a turbid medium with larger scattering particles. When an object hidden behind a turbid medium with larger scattering particles was imaged by the optical Kerr gated imaging technique, the image contrast would become worse due to the influence of residual multiply scattered photons.

Finally, we simulated the temporal and spatial evolution of a femtosecond pulse transmitted through turbid media with different thicknesses with the OD = 11. The turbid media used here were composed of 0.7 μm polystyrene microspheres, the thicknesses of which were set to be 1 and 5 cm, respectively. Figures 8(a) and (b) show the intensity distributions of the transmitted pulse on the front faces of the turbid media. As shown in figures 8(a) and (b), the FWHMs of the intensity distributions of the transmitted pulses are equal to 1 and 1.9 cm for $l = 1$ cm and $l = 5$ cm, respectively. From figures 8(a) and (b), we can see that the femtosecond pulse transmitted through the turbid medium was diffused seriously, and the number of transmitted photons collected on the front face decreased with increase of the thickness of the turbid medium. Thus, for direct imaging of an object hidden behind a

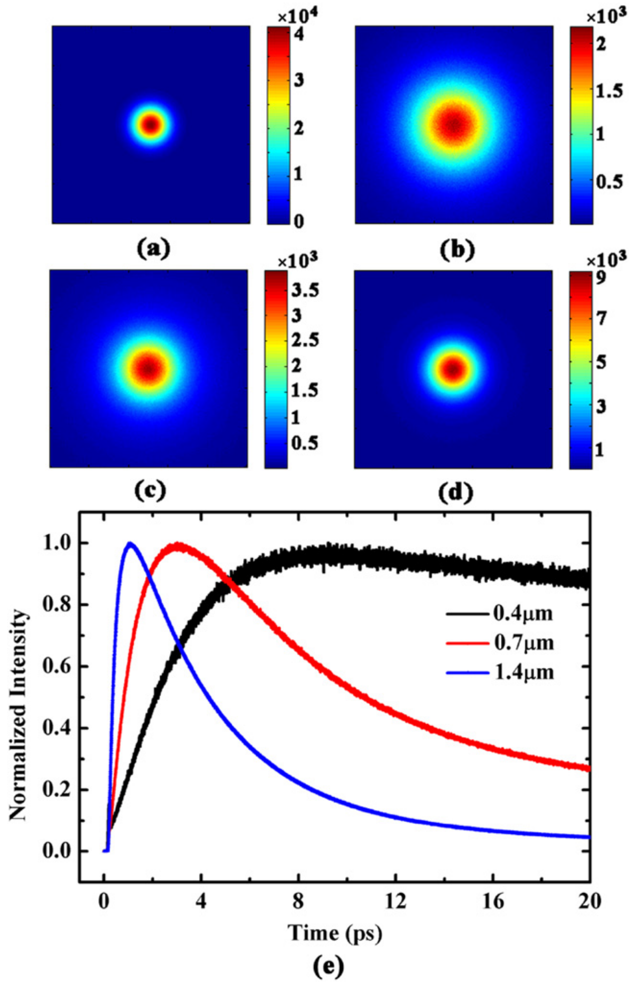

Figure 7. Simulation of spatial intensity distributions and temporal intensity profiles of a femtosecond pulse transmitted through turbid media with different sizes of the scattering particles. (a) The intensity distribution of the incident pulse. (b)–(d) The intensity distributions of the transmitted femtosecond pulse on the front faces of the turbid media of 0.4, 0.7 and 1.4 μm polystyrene microspheres, respectively. (e) The normalized temporal intensity profiles of the transmitted femtosecond pulse.

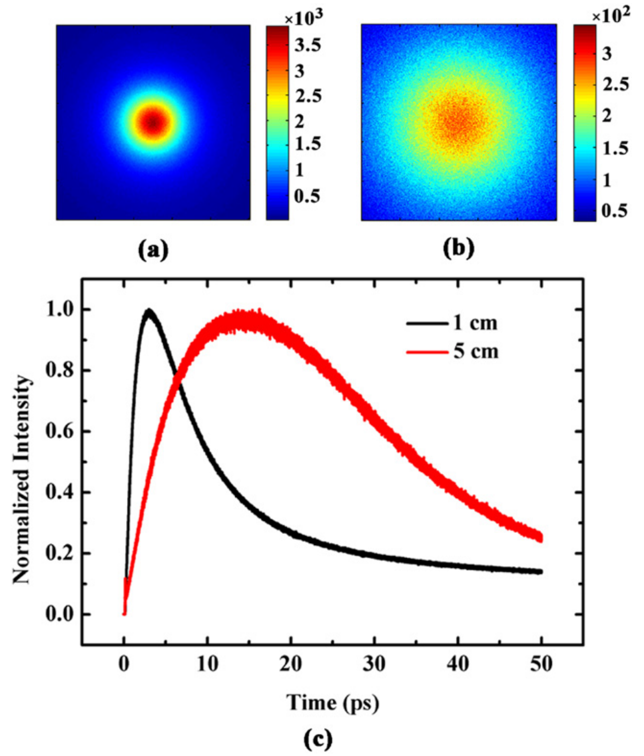

Figure 8. Simulation of the spatial intensity distributions and temporal intensity profiles of a femtosecond pulse transmitted through turbid media with different thicknesses. (a), (b) The intensity distributions of the transmitted pulse on the front faces of the 1 and 5 cm-thick solutions of 0.7 μm polystyrene microspheres, respectively. (c) The normalized temporal intensity profiles of the transmitted femtosecond pulse.

turbid medium, with a thicker turbid medium at the same OD, the image contrast would become worse due to the greater number of forward scattered photons. Figure 8(c) shows the normalized temporal intensity profiles of the transmitted femtosecond pulse as shown in figures 8(a) and (b). From figure 8(c), we can see that the transmitted femtosecond pulse duration was broadened more by increasing the thickness of the turbid medium. Therefore, if the gating time of the OKG was longer than the temporal duration of the ballistic photons, the image contrast would become worse for objects hidden behind a thicker turbid medium of the same scattering particles and OD. These simulation results were in good consistency with the experimental results.

4. Conclusion

In summary, this work presents optical Kerr gated imaging of an object hidden behind a turbid medium using a femtosecond laser. We studied the influence of both the scattering particle size and the thickness of the turbid medium on the image contrast. The experimental results show that for a given OD, the image contrast of direct imaging decreases with increase of the scattering particle size or decrease of the thickness of the turbid medium. Compared with direct imaging, optical Kerr gated imaging has a better image contrast. Furthermore, we also studied the temporal and spatial evolution of a femtosecond pulse transmitted through a turbid medium by Monte Carlo simulations. The simulations showed that the transmitted femtosecond pulse has a more broadened pulse duration and a more diffuse intensity distribution when it transits through a turbid medium with smaller scattering particles or larger thickness at the same OD. The simulations indicated that the image contrast of direct imaging was worse when the femtosecond pulse transmitted through a thinner turbid medium with larger scattering particles at the same OD. A better image contrast can be acquired for optical Kerr gated imaging as it eliminates more scattered photons effectively. Qualitative comparisons between the experiments and Monte Carlo simulations show good agreement.

Acknowledgments

The authors gratefully acknowledge the financial support for this work provided by the National Science Foundation of China under Grant Nos 61235003 and 61205129, the

National Basic Research Program of China (973 Program) under Grant No. 2012CB921804 and the Natural Science Basic Research Plan in Shaanxi Province of China (Program No. 2012JQ8002).

References

[1] Wang L, Ho P P, Liu C, Zhang G and Alfano R R 1991 *Science* **253** 769–71
[2] Dunsby C and French P M W 2003 *J. Phys. D: Appl. Phys.* **36** R207–27
[3] Wang Q Z, Liang X, Wang L, Ho P P and Alfano R R 1995 *Opt. Lett.* **20** 1498–500
[4] Paciaroni M and Linne M 2004 *Appl. Opt.* **43** 5100–9
[5] Zevallos L M E, Gayen S K, Alrubaiee M and Alfano R R 2005 *Appl. Phys. Lett.* **86** 011115
[6] Yasui T, Minoshima K, Abraham E and Matsumoto H 2002 *Appl. Opt.* **41** 5191–4
[7] Linne M, Paciaroni M, Berrocal E and Sedarsky D 2009 *Proc. Combust. Inst.* **32** 2147–61
[8] Tan W, Yang Y, Si J, Tong J, Yi W, Chen F and Hou X 2010 *J. Appl. Phys.* **107** 043104
[9] Tong J, Yang Y, Si J, Tan W, Chen F, Yi W and Hou X 2011 *Opt. Eng.* **50** 043607
[10] Kervella M, d'Abzac F-X, Hache F, Hespel L and Dartigalongue T 2011 *Opt. Express* **20** 32–41
[11] Tong J, Tan W, Si J, Cheng F, Yi W and Hou X 2012 *Chin. Phys. Lett.* **29** 024207
[12] Guo Z, Kan Wan S, August D A, Ying J, Dunn S M and Semmlow J L 2006 *Comput. Biol. Med.* **36** 209–23
[13] Schulz G, Weitkamp T, Zanette I, Pfeiffer F, Beckmann F, David C, Rutishauser S, Reznikova E and Müller B 2010 *J. R. Soc. Interface* **7** 1665–76
[14] Niedre M J, de Kleine R, Aikawa E, Kirsch D G, Weissleder R and Ntziachristos V 2008 *Proc. Natl Acad. Sci. USA* **105** 19126–31
[15] Sedarsky D, Paciaroni M, Berrocal E, Petterson P, Zelina J, Gord J and Linne M 2010 *Exp. Fluids* **49** 391–408
[16] Sedarsky D, Gord J, Carter C, Meyer T R and Linne M A 2009 *Opt. Lett.* **34** 2748–50
[17] Schmidt J B, Schaefer Z D, Meyer T R, Roy S, Danczyk S A and Gord J R 2009 *Appl. Opt.* **48** B137–44
[18] Sedarsky D, Idlahcen S, Rozé C and Blaisot J B 2013 *Exp. Fluids* **54** 1–12
[19] Idlahcen S, Méès L, Rozé C, Girasole T and Blaisot J B 2009 *J. Opt. Soc. Am.* A **26** 1995–2004
[20] Sedarsky D, Berrocal E and Linne M 2010 *Opt. Express* **19** 1866–83
[21] Ramella-Roman J, Prahl S and Jacques S 2005 *Opt. Express* **13** 4420–38
[22] Berrocal E, Meglinski I V and Jermy M C 2005 *Opt. Express* **13** 9181–95
[23] Moon S, Kim D and Sim E 2008 *Appl. Opt.* **47** 336–45